AD-A130 612 WIDE DYNAMIC RANGE ARRAY DETECTOR FOR ABSORBANCE AND ROTATION SPECTROMETRY(U) MICHIGAN STATE UNIV EAST LANSING DEPT OF CHEMISTRY P J AIELLO ET AL. 05 JUL 83 1/1

UNCLASSIFIED TR-13 N00014-76-C-1092 F/G 7/4 NL

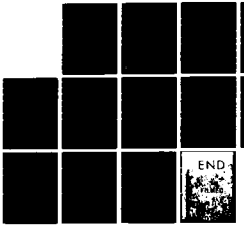

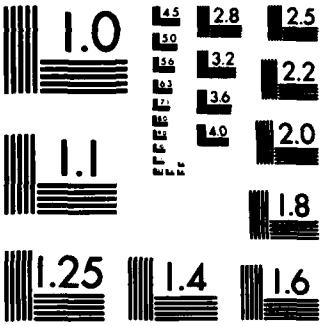

(12)

OFFICE OF NAVAL RESEARCH

Contract N00014-76-C-1092

Task No. NR 051-634

TECHNICAL REPORT NO. 13

WIDE DYNAMIC RANGE ARRAY DETECTOR FOR ABSORBANCE AND ROTATION SPECTROMETRY

by

Peter J. Aiello and Christie G. Enke

Prepared for Publication

in

American Chemical Society Symposium Series

Department of Chemistry
Michigan State University
East Lansing, MI 48824

July 5, 1983

SECURITY CLASSIFICATION OF THIS PAGE (When Data Entered)

REPORT DOCUMENTATION PAGE

READ INSTRUCTIONS BEFORE COMPLETING FORM

1. REPORT NUMBER: THIRTEEN	2. GOVT ACCESSION NO.: AD-A130 612
3. RECIPIENT'S CATALOG NUMBER:	
4. TITLE (and Subtitle): WIDE DYNAMIC RANGE ARRAY DETECTION FOR ABSORBANCE AND ROTATION SPECTROMETRY	5. TYPE OF REPORT & PERIOD COVERED: Interim Techical Report
	6. PERFORMING ORG. REPORT NUMBER:
7. AUTHOR(s): Peter J. Aiello and Christie G. Enke	8. CONTRACT OR GRANT NUMBER(s): N00014-76-C-1092
9. PERFORMING ORGANIZATION NAME AND ADDRESS: Chemistry Department, Michigan State University, East Lansing, MI 48824	10. PROGRAM ELEMENT, PROJECT, TASK AREA & WORK UNIT NUMBERS: NR 051-634
11. CONTROLLING OFFICE NAME AND ADDRESS: Chemistry Program, Office of Naval Research, Arlington, VA 22217	12. REPORT DATE: July 5, 1983
	13. NUMBER OF PAGES: 14
14. MONITORING AGENCY NAME & ADDRESS (if different from Controlling Office): ONR Representative, Ohio State University Research Center, 1314 Kinnear Road, Columbus, OH 43212	15. SECURITY CLASS. (of this report): Unclassified
	15a. DECLASSIFICATION/DOWNGRADING SCHEDULE:

16. DISTRIBUTION STATEMENT (of this Report)

Approved for public release, distribution unlimited.

17. DISTRIBUTION STATEMENT (of the abstract entered in Block 20, if different from Report)

18. SUPPLEMENTARY NOTES

19. KEY WORDS (Continue on reverse side if necessary and identify by block number)

20. ABSTRACT (Continue on reverse side if necessary and identify by block number)

Photodiode detectors have a limited dynamic range relative to a photomultiplier tube. Sensitivity (in terms of intensity) can be adjusted by changing the integration time, but the integration time for all diodes in array detector is the same for any given scan, and all portions of a spectrum are acquired within the same limited dynamic range. However, the results of scans taken at varying times can be combined to produce a data set with improved dynamic range. A microprocessor-controlled system for the automatic

DD FORM 1 JAN 73 1473 EDITION OF 1 NOV 65 IS OBSOLETE
S/N 0102-014-6601

SECURITY CLASSIFICATION OF THIS PAGE (When Data Entered)

sequencing of detector integration time and the storage of only the optimum readings is described. An improvement in dynamic range of 215 times that for a single integration time is theoretically possible, but in most systems, stray light and dark current will limit the practical dynamic range attainable.

WIDE DYNAMIC RANGE ARRAY DETECTOR FOR ABSORBANCE AND ROTATION SPECTROMETRY

PETER J. AIELLO[1] and CHRISTIE G. ENKE[2]

Department of Chemistry
Michigan State University
East Lansing, MI 48824

Photodiode detectors have a limited dynamic range relative to a photomultiplier tube. Sensitivity (in terms of intensity) can be adjusted by changing the integration time, but the integration time for all diodes in array detector is the same for any given scan, and all portions of a spectrum are acquired within the same limited dynamic range. However, the results of scans taken at varying times can be combined to produce a data set with improved dynamic range. A microprocessor-controlled system for the automatic sequencing of detector integration time and the storage of only the optimum readings is described. An improvement in dynamic range of 215 times that for a single integration time is theoretically possible, but in most systems, stray light and dark current will limit the practical dynamic range attainable.

Introduction and Review

Over the past decade, there has been considerable development in imaging type detectors for the measurement of ultraviolet (UV) and visible light. These new detectors have attracted the interest of a number of analytical spectroscopists. For absorption spectroscopy, analytical chemists have traditionally used such instruments as the photometer, which uses a narrow-band light source (for example the 254 nm emission line from a low pressure Hg lamp or a continuous source with a filter), a sample cell and a photomultiplier tube (PMT) as the detector. While useful for many specific applications, the single-wavelength photometer cannot determine multiple sample components simultaneously or provide a general absorbance characterization of the system. When information at multiple wavelengths is desired,

[1]Present address: Merck and Co., Inc., W1-10 Sumneytown Pike, West Point, PA 19486.

[2]Author to whom correspondence should be addressed.

a continuous source (such as a tungsten lamp) and a dispersive element (a prism or grating) is used. The dispersive element is mechanically rotated to vary the wavelength of light passed through a fixed exit slit. This selected monochromatic light beam then passes through the sample cell and is detected by a PMT. Spectrometers of this type maintain the single photometer's characteristics of wide dynamic range of absorbance, good sensitivity and rapid, linear response. In addition, they provide a continuous variation in the wavelength sampled with a relatively high degree of resolution in wavelength selection. Despite the great convenience and analytical power of the scanning spectrophotometer, it has two characteristics which are limiting in a number of areas of application. First, by sampling over only a narrow range of the dispersed light at any given time, it makes inefficient use of the optical information available and thus it prolongs the necessary measurement time. Second, because the wavelength must be physically scanned to provide measurements at multiple wavelengths, this data is acquired at different times. This limits its applicability in situations where the sample's optical properties are changing, particularly if the rate of such changes is an object of the measurement.

An obvious improvement in both these limitations could be achieved with simultaneous multiple wavelength detection. Of course, one would like to have such capability without sacrificing high resolution of wavelength selection, wide dynamic range and good sensitivity at all wavelengths, linear response, good geometric stability, no stray light, rapid response and rapid electronic readout. Unfortunately, no currently available multi-wavelength spectrometer has all these desirable properties.

Several spectrometers have been developed which use multiple detectors arranged in the focal plane of the dispersing element, thus achieving multi-wavelength detection. Multiple detectors are available in a variety of types and spatial geometries. These types of detectors include: the photographic plate, multiple PMT's (direct reader), the image dissector, the silicon vidicon, the charge-coupled device, the charge-injection device, and the photodiode array. The number of photosensitive elements in these detectors can vary from just a few to many thousands and these elements can be arranged linearly or in a two-dimensional array. As the number of elements increases, greater wavelength resolution is possible. When a linear array is placed in the focal plane, each element detects a different wavelength region. This is also true for two-dimensional arrays as the spectrometer entrance slit image is focused on a separate row of detectors for each wavelength region, and the signal from all elements in each row are averaged together. The two-dimensional array, however, has another advantage in that it can be used for two-dimensional applications such as Eschelle grating and streak camera images. Both linear and two-dimensional arrays are available with photosensitive elements of various dimensions. In general, the larger the element, the greater the dynamic range; the smaller the element, the greater the resolution. The ideal element dimensions

would match those of the spectrometer slit; i.e., narrow and tall for the best resolution and dynamic range. A discussion of a few types of multi-channel detectors, including a summary of their advantages and disadvantages follows.

The first multi-wavelength detector used was the photographic plate. It has several advantages: relatively easy channel identification, simple operation, low cost, integration over total exposure time, and availability in a wide variety of physical dimensions. Its disadvantages include limited dynamic range, non-linear response, difficult calibration and a very slow data retrieval procedure. Another type of multichannel detector in use is called the direct reader. This instrument uses multiple PMT's arranged across the focal plane of a polychromator (1). Many desirable characteristics are maintained through the use of the PMT detectors; however, the number of channels for a reasonably sized instrument is severely limited and the PMT's must be arranged at wavelengths appropriate for predetermined specific applications.

An early electronic scanning spectrometer utilized an image dissector as the detector (2). An image dissector is an electron multiplier which is sensitive to a small, electronically selectable region of a relatively large photocathode. The image dissector tube offers advantages such as high resolution, the absence of broadening effects of intense spectral lines and the capability of single photon counting (3). However, even though electronic wavelength scanning can be much faster than mechanical scanning, the image dissector does not provide simultaneous wavelength detection and light impinging on the unsampled area of the photocathode is lost. The single largest application of image dissector tubes is the measurement of low-light levels in astronomy (4).

The silicon vidicon (SV) has been widely used as a spectrometric detector. The development and characterization of vidicon spectrometers has been described in many recent papers (5-11). The light-sensitive surface of a vidicon tube is a two dimensional array of typically 500 by 500 pixels (picture elements). Absorbed photons reduce the charge stored in the pixel. The charge is restored by an electron beam focused on and scanned across the reverse side of the diode surface. The measured charging current at each pixel is proportional to the charge lost which is in turn related to the light intensity integrated over the interval between scans. Advantages of the SV include high scanning speed and large number of pixels. Disadvantages are serious, however. Wide dynamic range is not achievable at maximum resolution because blooming (adjacent pixel cross-talk) causes spectral line broadening. Sensitivity to UV light is low and incomplete readout or lag can be as high as 10% of the charge. For low light level spectroscopy a silicon intensified target tube (SIT) is used. With the SIT, as with the PMT, the sensitivity and spectral response are dependent on the choice of photocathode material. The SIT has been compared to the PMT for the measurement of transient fluorescent signals and has

been proven to provide comparable signal to noise ratios (S/N) (12,13).

Charge-Coupled Devices (CCD) are solid state imaging devices. These contain up to 500 x 500 pixels which provides moderate resolution. Lower resolution CCD's are less expensive than other solid state imaging devices (14,15). High can speeds are possible, the response is linear, and the dynamic range is about 1000. One significant feature of the frame transfer type of CCD detector is that all elements of the array integrate intensity during exactly the same time frame. The integration period is terminated by simultaneously transferring the integrated intensity signals to an analog shift register from which they are subsequently read out serially. Unfortunately, blooming and lag do occur if saturation is attained. Sensitivity is below that of a typical silicon device, in the UV region of the spectrum.

The charge-injection device (CID), a solid state imaging device in the developmental stage, has several unique features (16). One of these is its capability of nondestructive readout. With this capability, blooming (still a problem if saturation is attained) can be avoided by periodically scanning the array in a nondestructive readout mode. This mode can determine which pixels are near saturation. These pixels can then be selectively sampled in the normal destructive mode so that saturation is avoided while adjacent pixels with low incident light intensity can continue integrating. Another unique capability is that the integrated circuit is fabricated to allow random addressing of pixels. Therefore, faster readout speeds can be achieved if only a subset of the pixel information is required for a particular application.

The characteristics of silicon photodiode (SPD) arrays have been discussed in many recent papers (17-24). Over the last few years, self-scanned linear SPD arrays have been used for a number of analytical spectrochemical measurements (25-33). These arrays (called linear diode arrays or LDA) are currently available with up to 4096 photodiodes. It has been shown that LDA's have superior blooming and lag performance when compared to most other imaging type detectors (19,22). This allows the signal integrating capability of the array to become a very powerful asset. Since blooming does not occur, one can allow several photodiodes to saturate while adjacent photodiodes can integrate low light level signals. E.G.&G. Reticon (34) has made available LDA's specifically designed for spectroscopy. These arrays are self-scanned and provide real-time electronic readout with up to 1024 diodes. Each photodiode is a slit-shaped 25 μm wide by 2.5 mm high. This relatively large active area gives a dynamic range of up to 10,000 and the narrow width allows for excellent wavelength resolution. Although the arrays are much less sensitive than the PMT, useful measurements can be made over a region from 200 to 1000 nm. When improved sensitivity is needed, an electron multiplier type image intensifier can be used. These image intensifiers use an array of electron multipliers in a structure called a microchannel plate (MCP). Each channel in the MCP can provide a gain of up to six orders of magnitude (35).

Complete MCP's can be stacked to provide even higher gains. For response in the vacuum ultra-violet spectral region (50-200 nm) a SSANACON, self-scanned anode array with microchannel plate electron multiplier, has been used (36). This involves photoelectron multiplication through two MCP's, collection of the electrons directly on aluminum anodes and readout with standard diode array circuitry. In cases where analyte concentrations are well above conventional detection limits, multi-element analysis with multi-channel detectors by atomic emission has been demonstrated to be quite feasible (37). Spectral source profiling has also been done with photodiode arrays (27,29,31). In molecular spectrometry, imaging type detectors have been used in spectrophotometry, spectrofluometry and chemiluminescence (23,24,26,33). These detectors are often employed to monitor the output from an HPLC or GC (13,38,39,40).

Automatic Optimization of Integration Time

As indicated in the previous section, one of the most severe limitations of current imaging detectors is their dynamic range. The Reticon "S" series photodiode arrays have been shown to have a dynamic range of about 10,000 (22,34) for a single integration time. The conventional single channel detector, the photomultiplier tube (PMT), exceeds this dynamic range by more than 2 orders of magnitude. In order to extend the dynamic range of SPD detectors, the integration time (time between successive readings) can be varied. When SPD's are arranged in an array, the integration time for each diode is the time between the initiation of sequential scans of the array. Thus the integration time is unavoidably identical for each diode in the array for any given scan. In most analytical spectroscopy applications, however, no single integration time is optimum for every element (wavelength) in the array. Herein is described a solution to this problem which involves acquiring successive spectra at increasing integration times so that data taken at the optimum integration time for each photodiode is available.

The integrating capability of the linear diode array is achieved by charge integration, a technique which enhances the signal and averages the noise. This is very useful as the signal to noise ratio (S/N) under many conditions increases linearly with the integration time, whereas S/N enhancement by averaging replicate measurements increases only with the square root of the number of scans averaged (41,42). Therefore, the maximum resolution and S/N are obtained if each photodiode is allowed to integrate charge until it nears saturation. Figure 1 shows multiple spectra of a quartz halogen lamp taken with a Reticon 512S LDA at integration times of 5, 10, 20, 50, 200 and 500 ms. In each of these spectra, the detector dark current has been subtracted out. Because the dark current is also integrated, the saturation level for this integration of light current appears to decrease with increasing integration time. The total dynamic range is actually decreasing because of the increase in the

integrated dark current. The spectra shown in Figure 1 were obtained with the detector at room temperature. With the detector cooled to liquid nitrogen temperature, the useful maximum integration time is extended to about 24 h (19). It should also be noted that the profiles of these spectra are products of the polychromator transfer coefficient, the lamp spectral output and the detector sensitivity at each wavelength. At the shorter integration times, the photodiodes detecting the wavelengths above 500 nm are nearing saturation. At longer integration times the wavelengths near 300 nm are optimized (half-scale or larger). However, this is achieved at the expense of the information at the longer wavelengths which is now lost due to saturation of those photodiodes. In a normal LDA system, spectra are acquired at various trial integration times and then data are taken at the single integration time which is determined to be the best compromise. This usually results in a severe degradation of the photometric accuracy at those wavelengths for which the signal is weakest.

If different integration times are used for successive scans, the longest integration time scan will provide the best reading for the wavelength where the signal is weakest while the shorter integration time scans will give the best reading for those diodes that were saturated during the longer times. In our system, as shown in Figure 2, the integration time is doubled for each successive scan. The initial integration time, T, should be chosen such that no photodiode has neared saturation. If the integration time is doubled n times (in Figure 2, n=4), then the longest integration time is $2^n t$ and the total experimental time, T, will be

$$T = 2^{n+1}t - t$$

This means that data are acquired at the optimum integration time for each photodiode in a total time of approximately twice the longest integration time in the sequence. The optimum integration time is between 47.5% and 95% of saturation. The dynamic range improvement, D, will be

$$D = 2^{(n-1)}$$

assuming the dark current is negligible at the longest integration time used.

The number of integration time doublings, n, can be increased until either a time limitation imposed by the experiment is reached, or the integrated dark current exceeds 50% of saturation. The dark current can be reduced by cooling the LDA. The thermoelectric coolers used in our instrument cool the detector to a temperature of about -5 C which provides a maximum useful integration time of about 20 s.

It should be noted that as the integration time is increased, many of the photodiodes may reach saturation while adjacent photodiodes have yet to attain their optimum integration time.

This would be a significant problem in other imaging detectors such as CCD's, CID's and vidicons. In the case of these detectors, when saturation is reached, charge will leak from the saturated pixels (picture elements) to adjacent pixels. This "blooming" effect has been shown to be minimal in linear photodiode arrays (21,22). Thus integration times for which many photodiodes are saturated can be used while useful information is still obtained from the non-saturated photodiodes. This information will contain only the integrated light intensity for each photodiode, free of bleed-through from adjacent saturated photodiodes. The procedure by which the integration time is sequenced and only the optimum readings are stored is included in the instrument description below.

Instrument Optics

The optics of the instrument in which the multiple integration time array detector is implemented are described in this section. The goal of the instrument is to provide simultaneous absorbance and optical rotatory dispersion (ORD) measurements in the ultra-violet (UV) and visible spectral regions and to repeat this at very high speeds. An instrument capable of measuring simultaneously more than one physical property of a chemical system has great potential utility. Also such an instrument can assure that the properties measured actually refer to the same material under the same conditions. Figure 3 is a block diagram of the optical setup as configured for measurement of optical rotation and absorbance. The light source used is a 150 W xenon arc lamp. This high intensity is necessary when there is interest in the ultra-violet region of the spectrum because of the relatively low detector sensitivity at shorter wavelengths. The light then passes through a polarizer of the Glan-Thompson prism type. Linearly polarized light then passes through a sample cell which is 1 decimeter in length. If the sample is optically active, the plane of polarization is rotated by an amount that is wavelength dependent. The beam then passes through the analyzer. The analyzing polarizer is rotated under computer control in 0.01 degree increments. The light is then collected and focused by a lens onto the entrance slit of a spectrograph. The entrance slit of the spectrograph is interchangeable which allows the operator to make the best compromise between resolution and signal strength. A reflecting mirror simply folds the light path such that the inlet optics are physically separated from the spectral image produced. The light is then dispersed by a J-Y concave holographic grating. This grating (100 mm focal length, F/2.0) provides a flat-field image on the light sensitive region of the linear diode array detector. The grating has a reciprocal linear dispersion of 32 nm/mm resulting in a 400 nm wide spectral window to be viewed by the detector. The window which is viewed can be changed by physically sliding the detector back and forth in the focal plane. The low F number of the grating helps to maximize the light throughput of the spectrograph. The holographic grating

also serves to reduce stray light as the random error in groove position is virtually nonexistant.

The linear photodiode array (LDA) detector in this spectrometer is the RL512S made by Reticon (34). It has 512 photodiodes each 2.5 mm high and 25 μm wide. The LDA is self-scanned which provides real-time computer compatible serial electronic output for all 512 channels in succession. The detector is responsive over a range of 200-1000 nm. The array can be read out at very high speeds. At a 1 MHz clock frequency (the array can be clocked up to 10 MHz) data from successive channels appear every 4 μs, and the readout time of the complete LDA is only slightly greater than 2.0 ms. It should be noted that this is also the minimum integration time for a 1 MHz clock frequency. The integration time is extended by simply pausing for the desired length of time between readouts. The total integration time is the time from the initiation of the previous readout to the initiation of the current readout. The charge collected at each photodiode is directly proportional to the light intensity integrated over this time.

The Microcomputer and Data Acquisition System

It is apparent that the linear diode array detector can generate data at extremely high rates and that the data acquisition would best be done by computer. Rather than overburden a single minicomputer by interfacing several instruments to it, a single board computer was designed to give each instrument its own control and data acquisition capabilities. A particular single board computer (SBC) designed by Bruce Newcome (43) was used in the LDA spectrometer. The Intel 8085A microprocessor chip used in this microcomputer is powerful enough to fully control all instrument functions as well as to perform the data acquisition process. The system has been mechanically and electronically designed for easy interfacing. A block diagram of the microcomputer system excluding the LDA interface is shown in Figure 4. Ten K-bytes of programmable read-only memory (PROM) on the CPU bus contain the FORTH programming language. There are 22 K-bytes of random access memory (RAM) available for user program space. An interrupt controller is used for Input/Output (I/O) operations as well as data acquisition. Two universal synchronous/asynchronous receiver transmitters (USART) are used, the first for direct terminal I/O, the other for communication to a PDP 11/40 minicomputer. Also interfaced to the CPU bus is a dual floppy disk system. This provides storage space for both data and software. A local graphics monitor is used (256 by 256 pixel resolution) for initial data display. The CPU is also interfaced to a stepper motor which rotates the analyzer in the optical path in 0.01 degree increments.

Figure 5 is a block diagram showing the data acquisition hardware. Since the LDA is self-scanned, the only control the CPU can have on the LDA is to initiate the scan (readout) process. By controlling the timing of the initiation signal, the CPU controls

the integration time of the detector. The data acquisition is done completely in hardware when enabled by the CPU. Normally, when data are acquired at these high speeds, it is done by taking control of the CPU bus while putting the CPU on hold, and storing the data directly in RAM. This is called direct memory access (DMA). However, because the CPU is needed to program the integration time for the scan following the current readout, this straightforward approach could not be used. Instead, data are stored directly in RAM as in DMA, but the memory is not connected to the CPU bus when this is done. During data storage, the RAM is on the "data acquisition" bus. This RAM can be switched between the data acquisition bus and the CPU bus to allow the CPU access to the data after collection.

Each data point is stored in a 16-bit word; 12 bits for the ADC output, and 4 bits for the value of n (integration time doublings) for that conversion. On successive scans each at longer integration times, the converter output and n value overwrite the one taken for that channel on the previous scan, unless the ADC has overranged. ADC overrange occurs if the integrated charge exceeds 95% of the saturation value. Thus, at the end of the longest scan, one 512-word section of memory has the complete spectrum, each point having been recorded at its optimum integration time with the corresponding value of n.

There are actually two sections of RAM which under CPU control are exchanged between the CPU bus and the data acquisition bus. Since the CPU does not need to be inactive during acquisition, it can unload one RAM bank of data while the other is being filled with new data from the data acquisition bus.

Performance

In order to measure the practical dynamic range, the absorbance of a series of neutral density filters was measured. The measurements are all taken at 600 nm. The results are plotted in Figure 6. The initial integration time was 3 ms followed by 13 integration time doublings (14 readings) with the detector at -2 C. The longest integration time of 24.6 s was only slightly longer than the time in which the dark current saturates the array. The response is linear from about 0.0-4.2 absorbance units. For a nominal absorbance of 3.96, an absorbance of 4.03 was measured. This corresponds to a 2% error at an intensity 4 orders of magnitude below the maximum. The dynamic range is thus about 5×10^5. This could be improved considerably by using a 14-bit ADC to take advantage of the full dynamic range of the LDA (10^4), or by further cooling of the LDA to allow longer integration times.

Figure 7 shows, however, that with the current optics system, stray light causes significant deviations from Beer's Law in measurements of highly absorbing systems. The curve was acquired by measuring the absorbance of $KMnO_4$ solutions of known concentration using the LDA channel at λ = 545 nm. The Xe arc lamp was used and an IR cutoff filter was placed in the light path

in order to reduce stray light. Using a 12 ms integration time and 10 doublings (11 readings), samples with absorbances of greater than 2 at 545 nm do not result in the decrease in intensity at 545 nm diode expected because stray light of other wavelengths is hitting that photodiode. This problem is common to all array detector absorbance spectrometers where the light intensity varies greatly as a function of wavelength.

Stray light for this instrument was previously determined to be <0.004% (21). However, in an instrument of this type, order overlap and all internal reflections inside the polychromator cannot be eliminated through the use of a narrow bandpass filter as in a normal single wavelength spectrometer. The stray light problem is much worse in our system for short wavelength measurements than for long because both the source intensity and detector sensitivity decrease greatly toward the UV end of the spectrum. If stray light could be eliminated, absorbances up to 4.0 could be measured as demonstrated in Figure 6 where the experiment is not sensitive to stray light interference.

Figure 7 indicates that even with the presence of stray light, the system is quite useable over the critical absorbance range from 0 to 2. However, array detector spectroscopy would be greatly aided by the development of two new devices. One is a filter that would have an absorption spectrum that complements the source spectrum so that the combination would have more uniform spectral intensity. The other is a filter that would pass only the blue part of the spectrum in one region, only the red part in another and only the mid part in between. If such a filter were designed to match the dimensions of an array detector, and the dispersion of the monochromator, each detection element would only be sensitive to its appropriate wavelength. The resulting system would be like a dual monochromator, but would not entail the large losses involved in tandem dispersion systems.

Application to Multiwavelength ORD Spectrometry

The light intensity transmitted through two linear polarizers is a function of the incident light intensity and the $\cos^2$ of the angle at which the polarizers are set. If the intensity is measured while the analyzer is rotated continuously, the signal detected will vary sinusoidally between 0 (when the polarizers are crossed) and some maximum value with a frequency twice that of the rotation of the analyzer. If the sample shows absorption but not optical activity, the new maximum intensity value observed, I, will be lower than the value of I_{max} and the absorbance can easily be calculated. If the sample is optically active but does not absorb, the amplitude of the signal will not change ($I = I_{max}$) but a phase difference will be observed between the sample and the reference signals. The observed rotation is exactly equal to this phase difference. By recording the signal intensity at several analyzer positions, both the intensity and phase information are obtained. If this signal intensity is measured at all wavelengths

simultaneously, complete spectra for both the absorbance and ORD will be measured.

To implement these procedures with this instrument, several spectra are acquired at different angular positions of the analyzer. The data at each wavelength are fit to a $\cos^2$ function using a non-linear least squares algorithm (43) with only the frequency specified. The resulting peak-to-peak amplitude, phase and amplitude offset parameters are used to calculate the absorbance and ORD spectra. The resulting spectra for a 1.05% albumin solution are shown in Figure 8. The improvement in data collection rate afforded by the array detection make this system useful in following absorption and ORD changes for reaction rate or flow system monitoring applications.

Conclusions

Array detector spectrometry offers many advantages over scanning spectrometers, especially where near simultaneous information at multiple wavelengths is required. With suitable optics and electronics, the resolution and dynamic range of modern array detectors can match that of a medium resolution scanning monochromator and PMT. Sensitivity comparable to the PMT can also be obtained if an intensifier is used. Array detector spectrometers are somewhat more susceptible to stray light interferences than scanning monochromators because the baffling cannot be so exclusive and the use of switched in filters for various wavelength regions is precluded. Because of the many and proven advantages of this new technology, the years ahead should see great strides in both the technology and applications of array detector spectrometry.

Acknowledgements

This work was supported in part by Abbott Laboratories and the Office of Naval Research. Dr. Fritz S. Allen of the University of New Mexico provided very helpful suggestions concerning the ORD instrumentation.

Literature Cited

1. Willard; Merritt; Dean; Settle. "Instrumental Methods of Analysis"; Sixth Ed., D. Van Nostrand: New York, 1981; p. 165.
2. Harbor, R. A.; Sonnek, G. E. Applied Optics 1966, 5, 1039.
3. Danielsson, A.; Lindblom, P.; Soderman, E. Chimica Scripta 1974, 6, 5.
4. Boyce, P. B. Science 1977, 198, 143.
5. Milano, M. J.; Pardue, H. L. ; Cook, T. E.; Santini, R. E.; Margerum, D. W.; Raychera, J. Anal. Chem. 1974, 46, 374.
6. deHaseth, J. A.; Woodward, W. S.; Isenhour, T. L.; Anal. Chem. 1976, 48, 1513.
7. Cook, T. E.; Santini, R. E.; Pardue, H. L. Anal. Chem. 1977, 49, 871.
8. Neiman, T. A.; Enke, C. G. Anal. Chem. 1976, 48, 619.
9. Talmi, Y. Anal. Chem. 1975, 47, 658A.
10. Talmi, Y. Anal. Chem. 1975, 47, 697A.
11. Talmi, Y. Am. Lab. 1978, March, 79.
12. Cooney, R. P.; Vo-Dinh, T.; Walden, G.; Winefordner, J. D. Anal. Chem. 1977, 499, 1048.
13. Cooney, R. P.; Boutilier, G. D.; Winefordner, J. D. Anal. Chem. 1977, 49, 1048.
14. Ratzlaff, K. L.; Paul, S. L. Appl. Spec. 1979, 33, 240.
15. Ratzlaff, K. L. Anal. Chem. 1980, 52, 916.
16. Lewis, H. A.; Denton, M. B. J. Automatic Chem. 1980 August, Preprint.
17. Horlick, G.; Codding, E. G. Anal. Chem. 1973, 45, 1490.
18. Yates, D. A.; Kuwana, T. Anal. Chem. 1976, 48, 510.
19. Horlick, G. Appl. Spec. 1976, 30, 113.
20. Simpson, R. W. Rev. Sci. Instrum. 1979 50, 730.
21. Aiello, P. J. M.S. Thesis, Michigan St[illegible] University, 1980.
22. Talmi, Y.; Simpson, R. W. Appl. Optics [illegible]0, 19, 1401.
23. Marino, D. F.; Ingle, J. D. Jr. Anal. C[illegible]m. 1981, 53, 645.
24. Talmi, Y. Appl. Spec. 1982, 36, 1.
25. Chuang, F. S.; Natusch, D. F. S.; O'Keefe, K. R. Anal. Chem. 1981, 53, 645.
26. Milano, M. J.; Kim, K. Anal. Chem. 1977, 49, 555.
27. Franklin, M.; Baber, C.; Koirtyohann, S. R. Spectrochimica Acta 1976, 31, 589.
28. Horlick, G.; Codding, E. G. Appl. Spec. 1975, 29, 167.
29. Edmunds, T. E.; Horlick, G. Appl. Spec. 1977, 31, 536.
30. Talmi, Y.; Sieper, H. P.; Moenke-Bankenburg, L. Analytica Chimica 1981, 127, 71.
31. Blades, M. W.; Horlick, G. Appl. Spec. 1980, 34, 696.
32. Sandel, B. R.; Broadfoot, A. L. Appl. Optics 1976, 15, 3111.

33. Ryan, M. A.; Miller, R. J.; Ingle, J. D. Jr. Anal. Chem. 1978, 50, 1772.
34. "S-Series Solid State Linear Diode Array", E.G.&G. Reticon Brochure, 1978.
35. Eberhardt, E. H. Appl. Optics 1979, 18, 1418.
36. Broadfoot, A. L.; Sandel, B. R. Appl. Optics 1977, 16, 1533.
37. Felkel, H. L.; Pardue, H. L. Anal. Chem. 1978, 50, 602.
38. McDowell, A. E.; Pardue, H. L. Anal. Chem. 1977, 49, 1171.
39. Dessey, R. E.; Reynolds, W. D.; Nunn, W. G.; Titus, C. A.; Moler, G. F. Clin. Chem. 1976, 22, 1472.
40. Cooney, R. P.; Vo-Dinh, T.; Winefordner, J. D. Anal. Chim. Acta 1977, 89, 9.
41. Carlson, E. M. Ph.D. Thesis, Michigan State University, 1978.
42. McCord, T. B.; Franston, M. J. Appl. Optics 1978, 14, 1437.
43. Newcome, B., unpublished data.
44. Deming, W. E. "Statistical Adjustment of Data"; Wiley: New York, 1943.

Figure Captions

Figure 1. Spectrum of quartz-iodine lamp at various integration times (in milliseconds).

Figure 2. Scanning time sequence for multiple integration time array detector system.

Figure 3. Block diagram of the modular optical system arranged for multiwavelength measurement of optical rotation and absorbance.

Figure 4. Microcomputer control system block diagram.

Figure 5. Data acquisition system block diagram including the integration time sequencing and data packing hardware.

Figure 6. Measured absorbance vs the nominal absorbance of various combinations of neutral density filters.
Curve (B) shows the entire experimental range.
Curve (A) shows the part from 0-1A in greater detail.

Figure 7. Response vs. known absorbance of $KMnO_4$ solution at 545 nm.

Figure 8. Absorption (1) and rotation (2) spectra for 1.05% albumin solution.

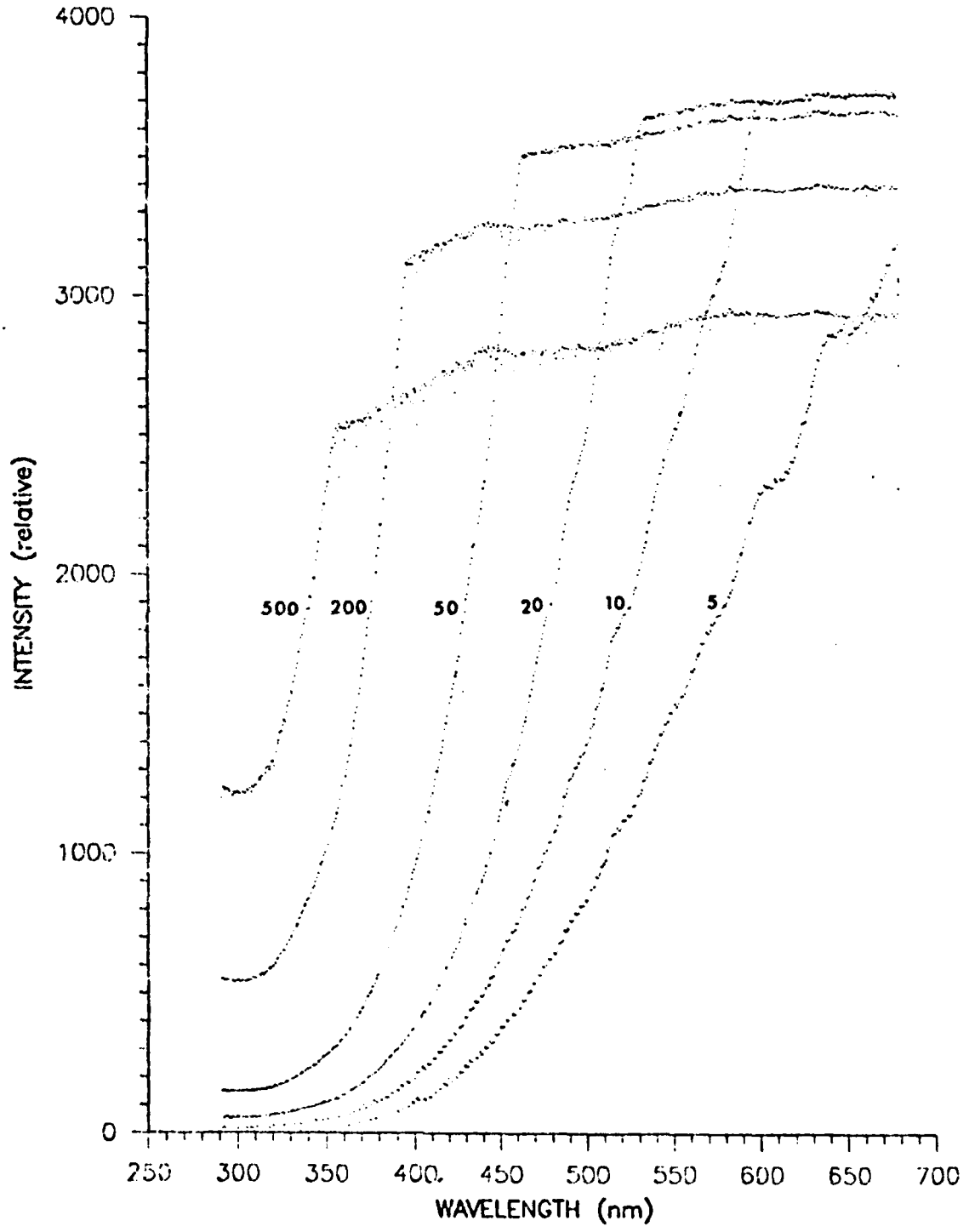
4000
3000
2000
1000
0
INTENSITY (relative)
500
200
50
20
10
5
250
300
350
400
450
500
550
600
650
700
WAVELENGTH (nm)

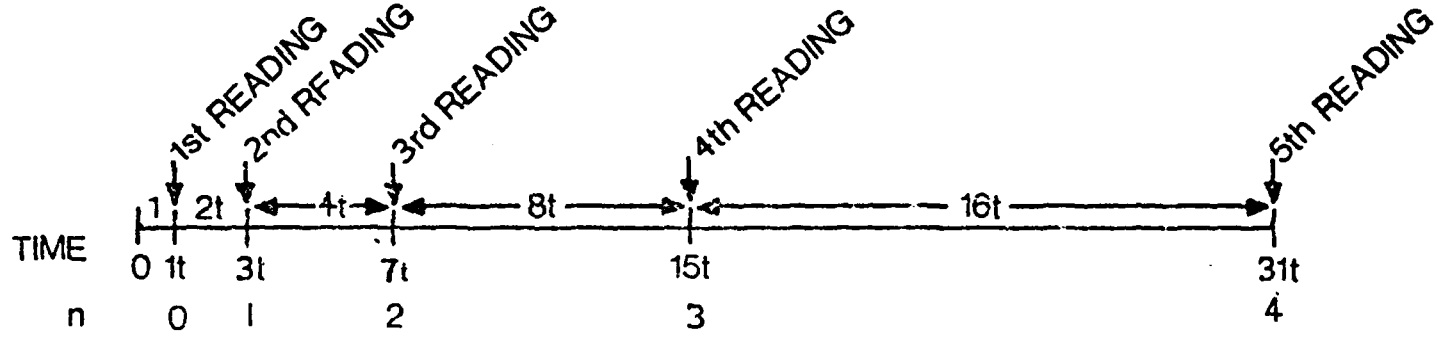

t = INTEGRATION TIME FOR MINIMUM SENSITIVITY

n = NUMBER OF INTEGRATION TIME DOUBLINGS = # Readings - 1

$2(2^n t) - t$ = TOTAL TIME FOR n DOUBLINGS

DYNAMIC RANGE IMPROVEMENT = $2^{(n-1)}$

EACH INTEGRATION TIME USES ALL BITS IN ADC

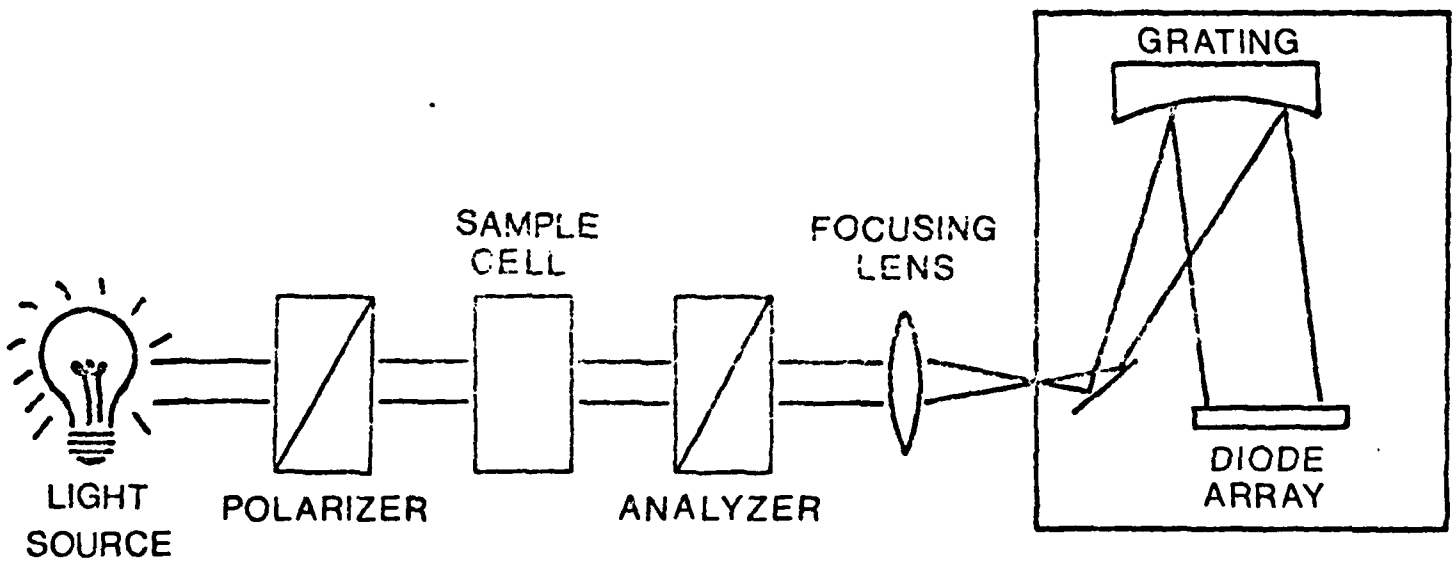
GRATING
SAMPLE CELL
FOCUSING LENS
LIGHT SOURCE
POLARIZER
ANALYZER
DIODE ARRAY

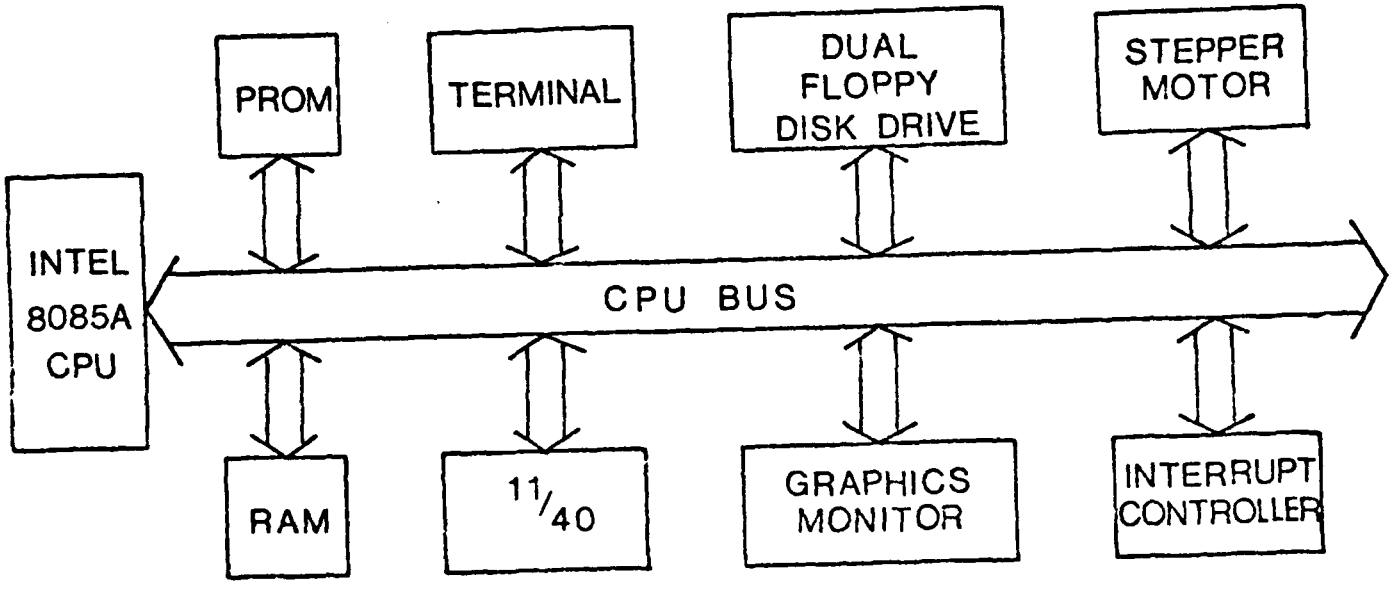
PROM
TERMINAL
DUAL
FLOPPY
DISK DRIVE
STEPPER
MOTOR
INTEL
8085A
CPU
CPU BUS
RAM
11/40
GRAPHICS
MONITOR
INTERRUPT
CONTROLLER

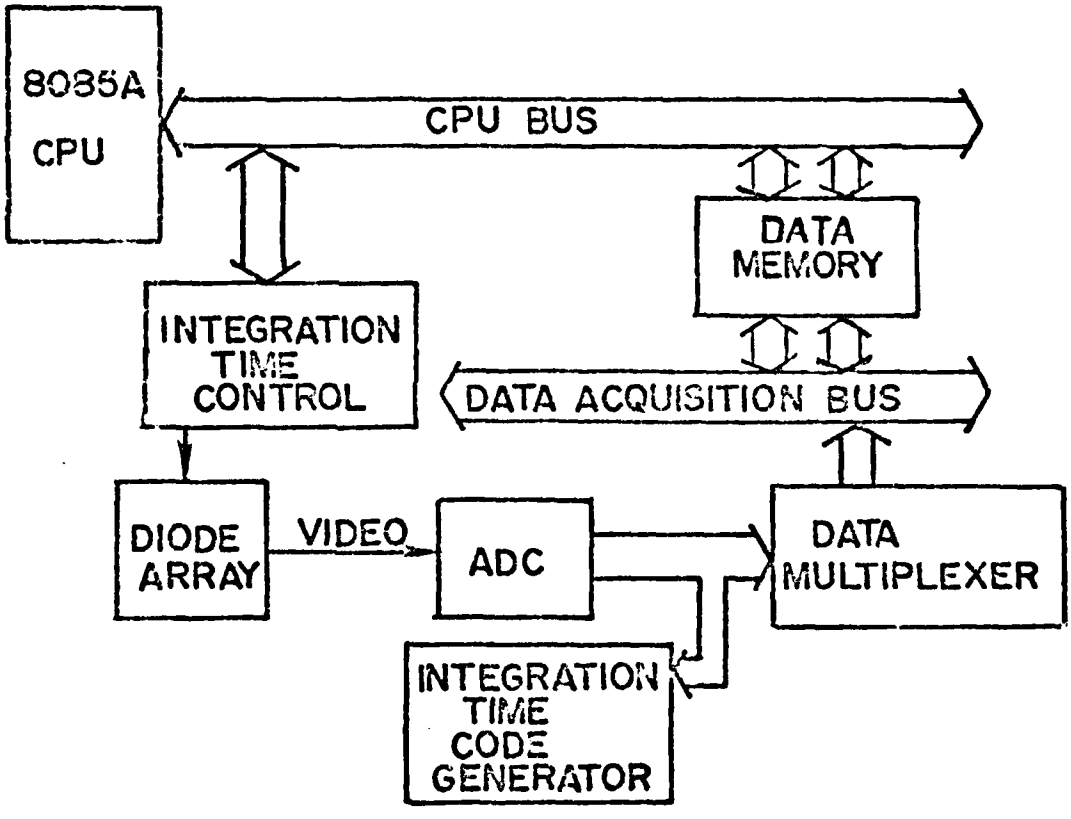
8085A
CPU
CPU BUS
DATA
MEMORY
INTEGRATION
TIME
CONTROL
DATA ACQUISITION BUS
DIODE
ARRAY
VIDEO
ADC
DATA
MULTIPLEXER
INTEGRATION
TIME
CODE
GENERATOR

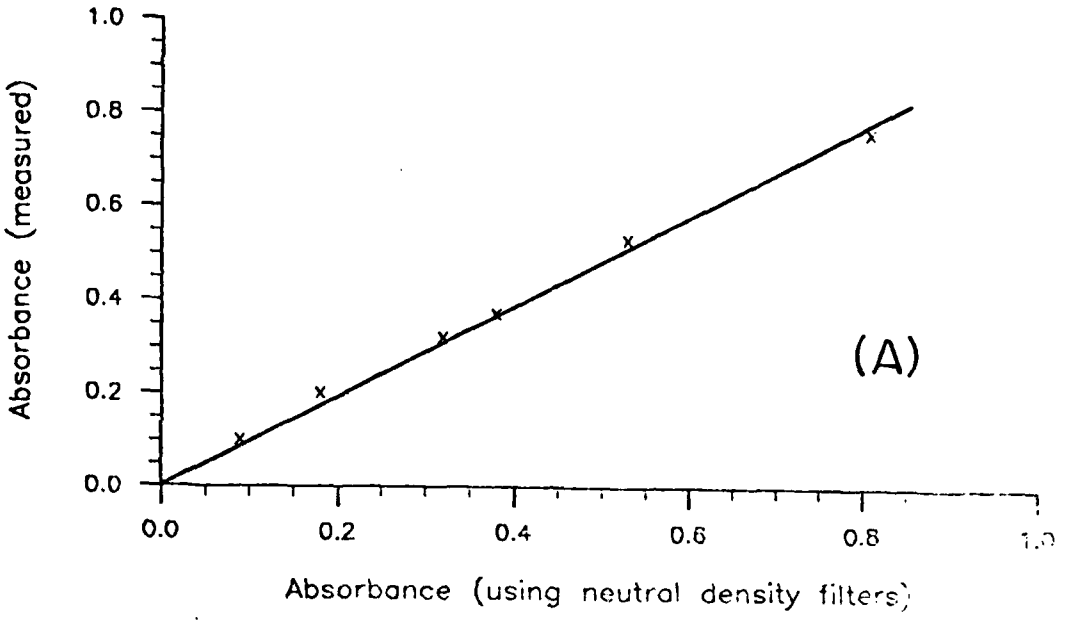
1.0
0.8
0.6
0.4
0.2
0.0
Absorbance (measured)
0.0
0.2
0.4
0.6
0.8
(A)
Absorbance (using neutral density filters)

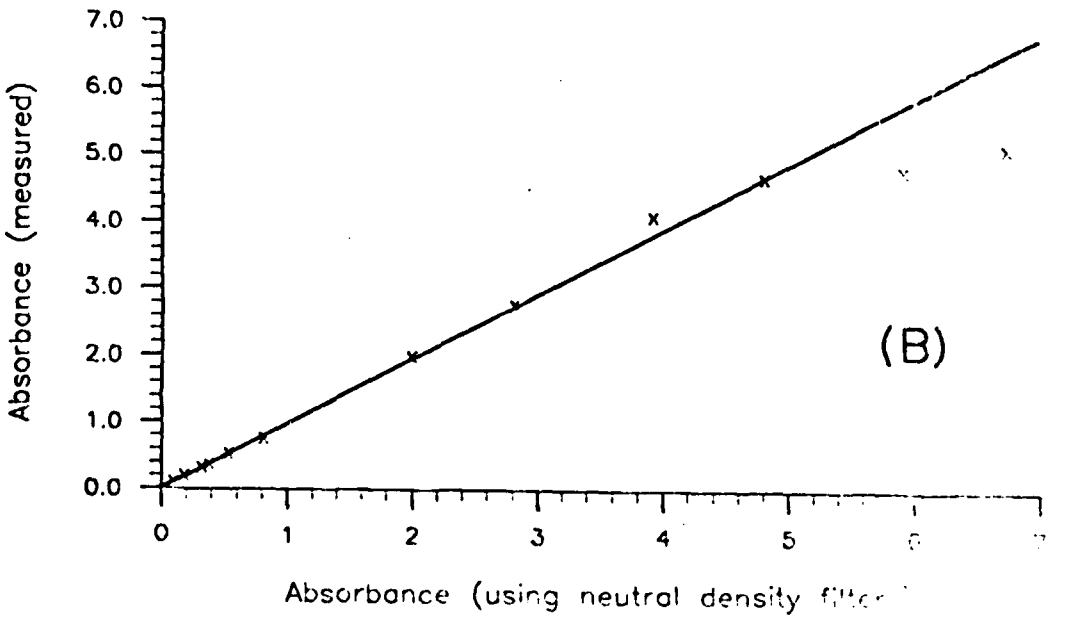
7.0
6.0
5.0
4.0
3.0
2.0
1.0
0.0
Absorbance (measured)
0
1
2
3
4
5
(B)

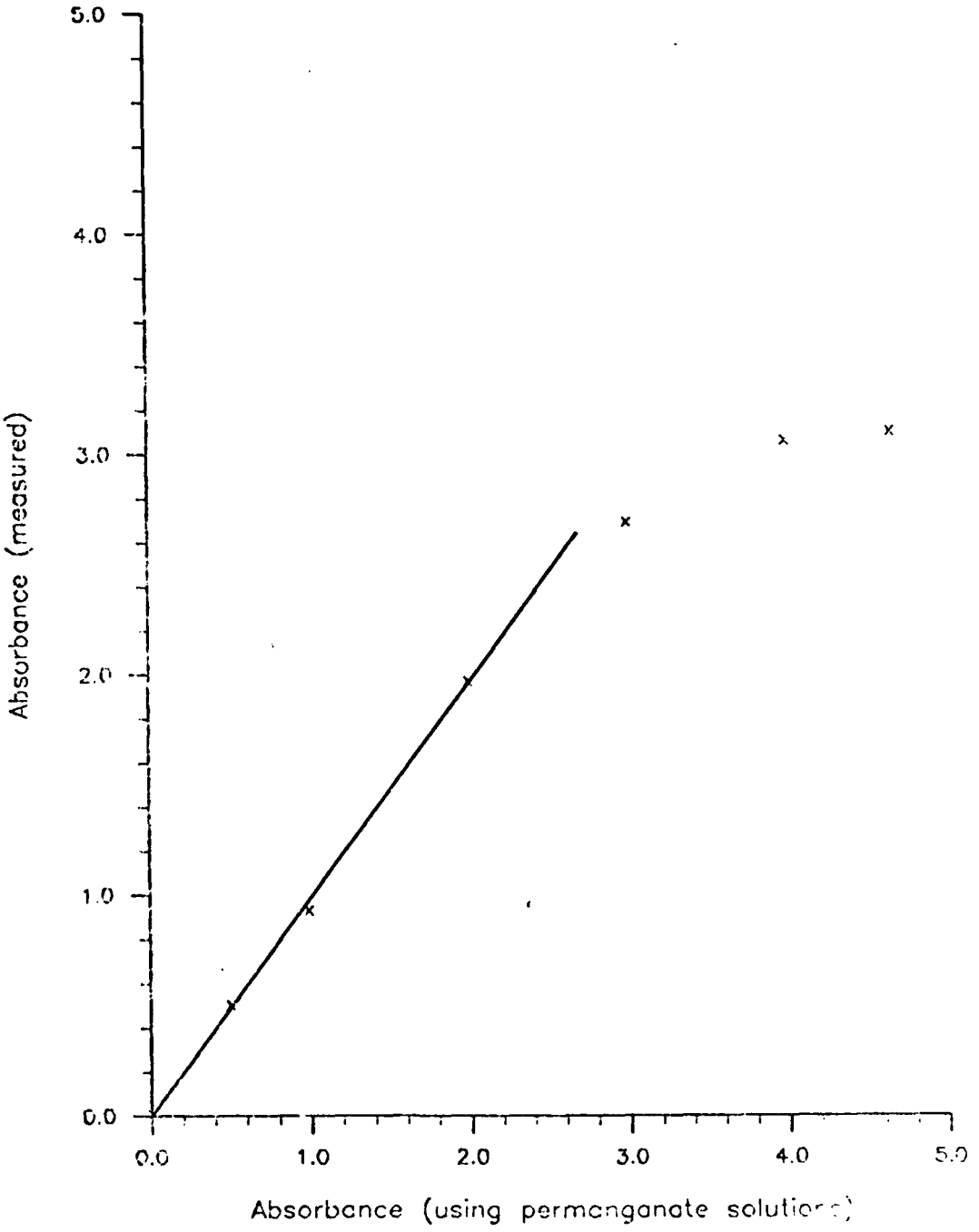
5.0
4.0
3.0
2.0
1.0
0.0
Absorbance (measured)
0.0
1.0
2.0
3.0
4.0
5.0
Absorbance (using permanganate solution)

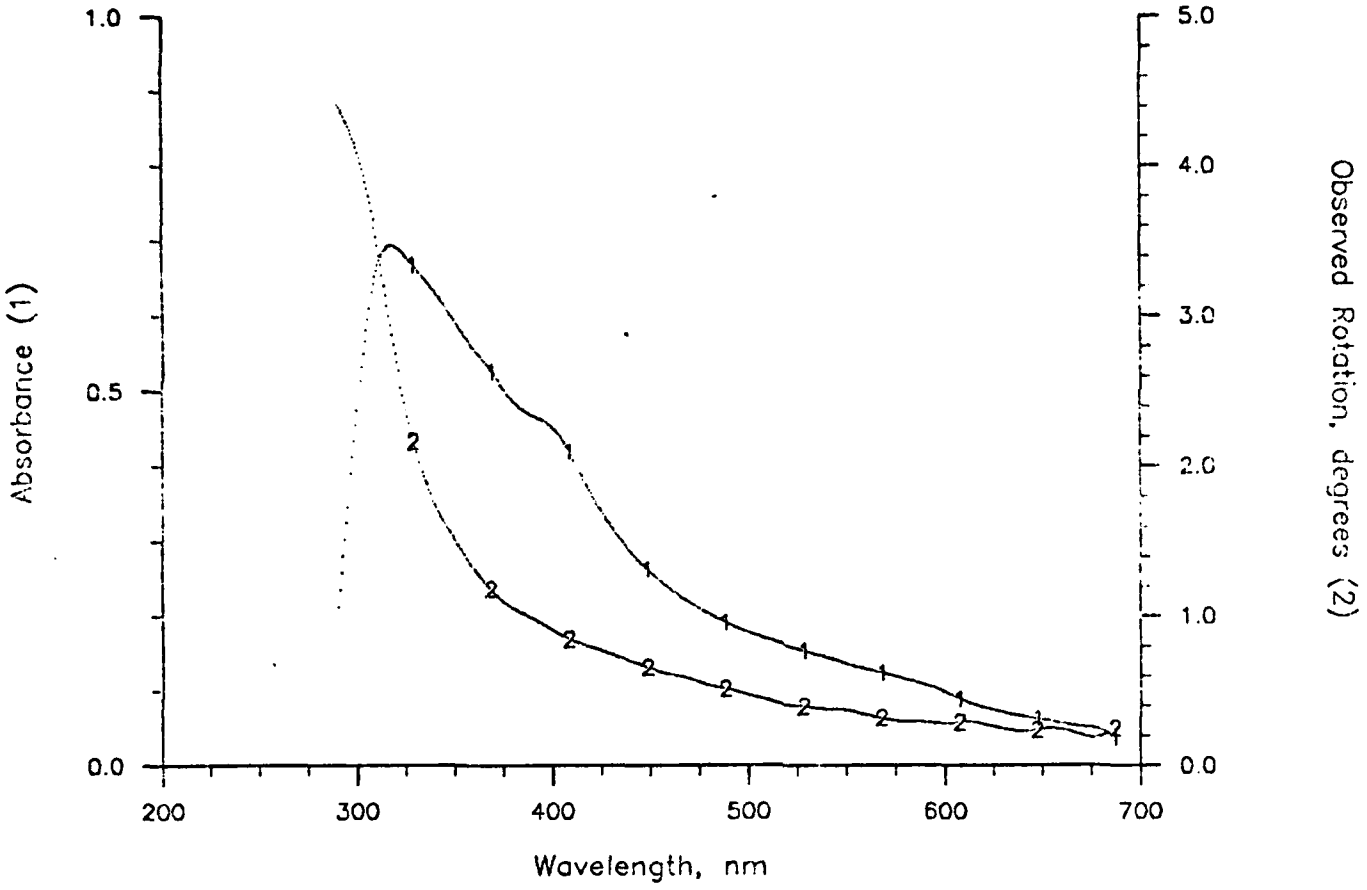
1.0
0.5
0.0
Absorbance (1)
5.0
4.0
3.0
2.0
1.0
0.0
Observed Rotation, degrees (2)
200
300
400
500
600
700
Wavelength, nm

4/82

472:GAN:716-4
94/GEN

TECHNICAL REPORT DISTRIBUTION LIST, GEN

	No. Copies
Office of Naval Research Attn: Code 413 800 North Quincy Street Arlington, Virginia 22217	2
ONR Pasadena Detachment Attn: Dr. R. J. Marcus 1030 East Green Street Pasadena, California 91106	1
Commander, Naval Air Systems Command Attn: Code 310C (H. Rosenwasser) Department of the Navy Washington, D.C. 20360	1
Defense Technical Information Center Building 5, Cameron Station Alexandria, Virginia 22314	12
Dr. Fred Saalfeld Chemistry Division, Code 6100 Naval Research Laboratory Washington, D.C. 20375	1
U.S. Army Research Office Attn: CRD-AA-IP P. O. Box 12211 Research Triangle Park, N.C. 27709	1
Mr. Vincent Schaper DTNSRDC Code 2803 Annapolis, Maryland 21402	1
Naval Ocean Systems Center Attn: Dr. S. Yamamoto Marine Sciences Division San Diego, California 91232	1
Naval Ocean Systems Center Attn: Mr. Joe McCartney San Diego, California 92152	1
Naval Weapons Center Attn: Dr. A. B. Amster, Chemistry Division China Lake, California 93555	1
Naval Civil Engineering Laboratory Attn: Dr. R. W. Drisko Port Hueneme, California 93401	1
Dean William Tolles Naval Postgraduate School Monterey, California 93940	1
Scientific Advisor Commandant of the Marine Corps (Code RD-1) Washington, D.C. 20380	1
Naval Ship Research and Development Center Attn: Dr. G. Bosmajian, Applied Chemistry Division Annapolis, Maryland 21401	1
Mr. John Boyle Materials Branch Naval Ship Engineering Center Philadelphia, Pennsylvania 19112	1
Mr. A. M. Anzalone Administrative Librarian PLASTEC/ARRADCOM Bldg 3401 Dover, New Jersey 07801	1

TECHNICAL REPORT DISTRIBUTION LIST, 051C

	No. Copies
Dr. M. B. Denton Department of Chemistry University of Arizona Tucson, Arizona 85721	1
Dr. R. A. Osteryoung Department of Chemistry State University of New York at Buffalo Buffalo, New York 14214	1
Dr. J. Osteryoung Department of Chemistry State University of New York Buffalo, New York 14214	1
Dr. B. R. Kowalski Department of Chemistry University of Washington Seattle, Washington 98105	1
Dr. S. P. Perone Department of Chemistry Purdue University Lafayette, Indiana 47907	1
Dr. D. L. Venezky Naval Research Laboratory Code 6130 Washington, D.C. 20375	1
Dr. H. Freiser Department of Chemistry University of Arizona Tucson, Arizona 85721	
Dr. H. Chernoff Department of Mathematics Massachusetts Institute of Technology Cambridge, Massachusetts 02139	1
Dr. A. Zirino Naval Undersea Center San Diego, California 92132	1
Dr. L. Jarris Code 6100 Naval Research Laboratory Washington, D.C. 20375	1
Dr. John Duffin, Code 62 Dn United States Naval Postgraduate School Monterey, California 93940	1
Dr. G. M. Hieftje Department of Chemistry Indiana University Bloomington, Indiana 47401	1
Dr. Victor L. Rehn Naval Weapons Center Code 3813 China Lake, California 93555	1
Dr. Christie G. Enke Michigan State University Department of Chemistry East Lansing, Michigan 48824	1
Dr. Kent Eisentraut, MBT Air Force Materials Laboratory Wright-Patterson AFB, Ohio 45433	1
Walter G. Cox, Code 3632 Naval Underwater Systems Center Building 148 Newport, Rhode Island 02840	1
Professor Isiah M. Warner Department of Chemistry Emory University Atlanta, Georgia 30322	
Professor George H. Morrison Department of Chemistry Cornell University Ithaca, New York 14853	1

TECHNICAL REPORT DISTRIBUTION LIST, 051C

	No. Copies	No. Copies
Professor J. Janata Department of Bioengineering University of Utah Salt Lake City, Utah 84112	1	
Dr. Carl Heller Naval Weapons Center China Lake, California 93555	1	
Dr. Denton Elliott AFOSR/NC Bolling AFB Washington, D.C. 20362		
Dr. J. Decorpo NAVSEA-05R14 Washington, D.C. 20362		
Dr. B. E. Spielvogel Inorganic and Analytical Branch P. O. Box 12211 Research Triangle Park, NC 27709		
Dr. Charles Anderson Analytical Chemistry Division Athens Environmental Lab. College Station Road Athens, Georgia 30613		
Dr. Samual P. Perone L-326 LLNL Box 808 Livermore, California 94550		
Dr. B. E. Douda Chemical Sciences Branch Code 4052 Naval Weapons Support Center Crane, Indiana 47522		
Ms. Ann De Witt Material Science Department 160 Fieldcrest Avenue Raritan Center Edison, New Jersey 08818		

TECHNICAL REPORT DISTRIBUTION LIST, 051D

	No. Copies	No. Copies
Dr. Henry Freiser University Department University of Arizona Tucson, Arizona 85721	1	
Dr. Lynn Jarvis Code 6170 Naval Research Laboratory Washington, D.C. 20375	1	
Dr. Gregory D. Botsaris Department of Chemical Engineering Tufts University Medford, Massachusetts 02155	1	
Dr. J. H. Hargis Department of Chemistry Auburn University, Alabama 36849	1	
Dr. Carl Heller Code 3851 Naval Weapons Center China Lake, California 93555	1	
Dr. Christie G. Enke Department of Chemistry Michigan State University East Lansing, Michigan 48824	1	

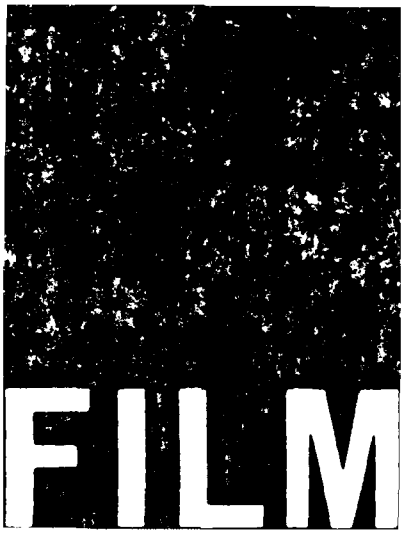
FILM